Hindawi
Complexity
Volume 2020, Article ID 8905031, 10 pages
https://doi.org/10.1155/2020/8905031

Research Article

Computation of Time Delay Stability Margin for the Automated Vehicular Platoon

Xunxun Zhang[1,2] **Li Li**[3] **and Xu Zhu**[4]

[1]*School of Civil Engineering, Xi'an University of Architecture and Technology, Xi'an 710055, China*
[2]*National Experimental Teaching Center for Civil Engineering Virtual Simulation (XAUAT), Xi'an University of Architecture and Technology, Xi'an 710055, China*
[3]*College of Computer and Information Engineering, Tianjin Normal University, Tianjin 300387, China*
[4]*School of Electronic and Control Engineering, Chang'an University, Xi'an 710064, China*

Correspondence should be addressed to Li Li; meggie_li@163.com

Received 29 November 2019; Revised 5 March 2020; Accepted 12 March 2020; Published 10 April 2020

Academic Editor: Honglei Xu

Due to the limited band width and congestion of communication channels in the wireless vehicle-to-vehicle (V2V) communication, time delay inevitably arises and dramatically leads to the disturbances for the automated vehicular platoon. This paper focuses on computing the exact time delay stability margin. In this study, we treat this problem as a stability issue of a consensus system with time delay, where each vehicle in the platoon is recognized as a node, and the interconnected information flow is represented as a graph. Then, the distributed controller is designed by combining the states of the vehicle itself and its neighbouring vehicles. Furthermore, the stability of the entire platoon is analysed according to the characteristic equation of the closed-loop system, and a necessary and sufficient condition for the exact time delay stability margin is obtained. Especially, for the automated vehicular platoon with undirected topology, it is revealed that exact time delay stability margin is determined by the largest eigenvalue of the augmented Laplacian matrix. Furthermore, a rapid method for finding exact time delay stability margin is proposed. Finally, numerical simulations demonstrate that this work generates exact and satisfactory time delay stability margin for the automated vehicular platoon.

1. Introduction

Vehicular platoon is a vital component of intelligent vehicle infrastructure cooperative systems (IVICS), which is the frontier of intelligent transportation system (ITS) [1]. An automated vehicular platoon consists of a group of coordinated vehicles, which move at an identical speed and maintain a prespecified formation geometry. Due to team cooperation, the automated vehicular platoon is conductive to improving traffic capacity, enhancing highway safety, and reducing exhaust emission and fuel consumption [2].

Recently, the automated vehicular platoon technology has attracted considerable attentions [3–6], which can be recognized as a combination of four components, i.e., vehicular longitudinal dynamics, interconnected information flow, distributed controllers, and intervehicle spacing policy [7, 8]. First, the vehicular longitudinal dynamics describes the dominant longitudinal behaviour of each vehicle. Second, the interconnected information flow depicts how the vehicles in the vehicular platoon exchange state information with the others. While its physical implementation depends on wireless vehicle-to-vehicle (V2V) and vehicle-to-infrastructure (V2I) communication [9]. Moreover, the structure of interconnected information flow can be classified into two types in terms of undirected and directed topologies. Third, the distributed controllers are utilized for the specific feedback control of each vehicle. Most controllers are linear [7, 10]. Fourth, the intervehicle spacing policy arranges the desired distance between the two successive vehicles and further determines the formation geometry.

In an automated vehicular platoon, the interconnected information flow depends on wireless communication. Due

to the limited band width and congestion of the communication channels, it is inevitable to introduce time delay to the vehicular platoon [11, 12]. Meanwhile, the time delay is the inherent phenomenon in the wireless communication networks, which is universally acknowledged as the main factor for the vehicular platoon and leads to string instability [13]. Therefore, it is of high importance to study the vehicular platoon with time delay. Therein, we focus on the computation of time delay stability margin for the automated vehicular platoon under both undirected and directed topologies.

To obtain the time delay stability margin, most literatures analyse the closed-loop system of the vehicular platoon and recognize the entire vehicular platoon as a consensus system [14]. For the stability analysis problem of the consensus system with time delay, the majority of the existing studies usually utilize Lyapunov-Krasovskii methodology [15, 16], Lyapunov–Razumikin methodology [12, 17], and generalised Nyquist criterion [18, 19]. However, these studies can provide only sufficient conditions, which are relatively conservative and fail to find the exact time delay stability margin. On the contrary, because these results mainly rely on some linear matrix inequalities, they are usually imprecise and cumbersome to deploy.

Motivated by this fact, we focus on offering an analytical method to find the exact time delay stability margin for the automated vehicular platoon under both the directed and undirected topologies. Therein, a second-order consensus system is used for modelling the longitudinal dynamics of the vehicular platoon, designing the control gains, and describing the interconnected information flow. By investigating the distribution of the roots for the closed-loop system's characteristic equation, we provide a necessary and sufficient condition for the stability of the vehicular platoon. Then, on the basis of the necessary and sufficient condition, the exact time delay stability margin can be found. Specially, for the undirected topology, by analysing the monotonicity relationship between each eigenvalue of the augmented Laplacian matrix and its corresponding time delay, it is revealed that the exact time delay stability margin is determined by the largest eigenvalue. Therefore, a more rapid method for computing the exact time delay stability margin is further proposed for the undirected topology.

In a word, the main contributions of this work are twofold. Firstly, to the best of the authors' knowledge, it is the first time that the exact time delay stability margin is analytically acquired for the second-order platoon. The exact time delay stability margin is obtained by searching the pure imaginary roots of the characteristic equation for the closed-loop system, and it is further demonstrated that only the positive pure imaginary root should be taken into consideration. Secondly, for the undirected topology, we originally propose a simple and rapid method to calculate the exact time delay stability margin. Only one time delay, which corresponds to the largest eigenvalue of the augmented Laplacian matrix, needs to be computed. Therefore, it is unnecessary to compute the delays for the other eigenvalues. For the large-scale vehicular platoon, the second contribution is particularly useful to dramatically reduce the computational burden.

The remainder of this paper is organised as follows. The problem statement is presented in Section 2. The computation of time delay stability margin for the automated vehicular platoon is elaborated in Section 3. In Section 4, numerical simulations are provided to demonstrate the validity and superiority of the proposed algorithm. Finally, the conclusions are summarized in Section 5.

2. Problem Statement

For the automated vehicular platoon, it can be treated as a combination of four components, *i.e.*, vehicular longitudinal dynamics, interconnected information flow, distributed controllers, and intervehicle spacing policy. In this part, the four components will be elaborately described, respectively.

2.1. Model for Interconnected Information Flow. In our work, we consider the platoon with $N + 1$ identical interconnected vehicles, including one leader and N followers. There are two typical interconnected information flows in terms of undirected and directed topologies. For the undirected topology (as depicted in Figure 1(a)), except that the leader vehicle transmits to the follower vehicles, the follower vehicles share state information with their neighbouring vehicles. For the directed topology (as depicted in Figure 1(b)), the vehicle receives the state information only from the following and the preceding vehicle. According to graph theory, there are some distinct properties between these two kinds of topologies. Especially, it is easier to analyse the stability of undirected topology.

For both the undirected and directed topologies, the interconnected information flow among the followers can be modelled by a graph $\mathcal{G} = \{\mathcal{V}, \mathcal{E}, \mathcal{A}\}$, where each vehicle is recognized as a node. $\mathcal{V} = \{1, 2, \ldots, N\}$ is the set of nodes and $\mathcal{E} \subseteq \mathcal{V} \times \mathcal{V}$ is the set of edges. The adjacency matrix associated with the graph $\mathcal{G}$ is characterized by $\mathcal{A} = [a_{ij}]_{N\times N}$, where $i, j \in \mathcal{V}$. The nonnegative adjacency weight $a_{ij} = 1$ means that the node i can get information from the node j; otherwise, $a_{ij} = 0$. Moreover, we assume that $a_{ii} = 0$ (no self-loop is allowed unless otherwise indicated).

To model the interconnected information flow between the leader and the followers, an augmented graph is defined as $\widetilde{\mathcal{G}} = \left\{\widetilde{\mathcal{V}}, \widetilde{\mathcal{E}}, \widetilde{\mathcal{A}}\right\}$, where $\widetilde{\mathcal{V}} = \{0, 1, 2, \ldots, N\}$ is the set of nodes including the leader and followers, and the index 0 represents the leader vehicle. $\widetilde{\mathcal{E}} \subseteq \widetilde{\mathcal{V}} \times \widetilde{\mathcal{V}}$ is the edge set appended with the information flow from the leader to the followers, and $\widetilde{\mathcal{A}}$ is the augmented adjacency matrix.

After modelling the interconnected information flow, we aim to describe its property with the graphs $\mathcal{G}$ and $\widetilde{\mathcal{G}}$. Therefore, two important matrices (*i.e.,* Laplacian matrix and pinning matrix) are introduced as follows. Firstly, the Laplacian matrix $\mathcal{L} = [l_{ij}]_{N\times N}$, which is associated with the graph $\mathcal{G}$, is defined as

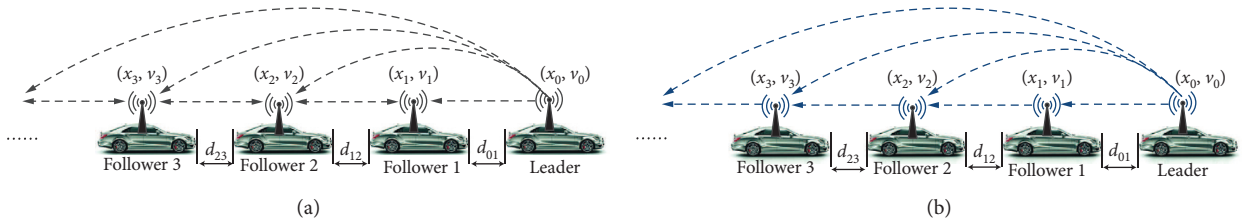

Figure 1: Typical interconnected information flow for vehicular platoons. (a) Undirected topology. (b) Directed topology.

$$l_{ij} = \begin{cases} -a_{ij}, & i \neq j, \\ \sum_{k=1}^{N} a_{ik}, & i = j. \end{cases} \tag{1}$$

Secondly, the pinning matrix $\mathscr{P}$, which is associated with the augmented graph $\widetilde{\mathscr{G}}$ characterizing the interconnected information flow from the leader to the followers, is defined as

$$\mathscr{P} = \text{diag}\{p_1, p_2, \ldots, p_N\}, \tag{2}$$

where $p_i = 1$ if the edge $\{i, 0\} \in \widetilde{\mathscr{E}}$; otherwise, $p_i = 0$. The expression $p_i = 1$ means that the ith vehicle can get information from the leader. p_i is called pinning gain in the field of complex networks [20]. If $p_i = 1$, the vehicle i is said to be pinned to the leader.

According to the algebraic graph theory [21], the augmented graph $\widetilde{\mathscr{G}}$ should contain at least one spanning tree rooting from the leader vehicle if the vehicular platoon is asymptotically stable. A spanning tree is an algebraic tree formed by some or all the edges of the augmented graph $\widetilde{\mathscr{G}}$ that links all the nodes. The graph $\widetilde{\mathscr{G}}$ containing a spanning tree means that a subset of its edges forms a spanning tree. Therefore, for a stable vehicular platoon, there should exist at least one directed path from the leader to each follower. In contrary, each follower can acquire information from the leader directly or indirectly.

2.2. Vehicle Longitudinal Dynamics. For the longitudinal dynamics of each vehicle, it is mathematically charactered by a second-order linear model. Moreover, to reduce the model complexity, the input-output feedback linearisation is applied to build the model. Then, the longitudinal dynamics of the ith vehicle are denoted by

$$\begin{cases} \dot{r}_i = v_i(t), \\ \dot{v}_i = u_i(t), \end{cases} \tag{3}$$

where r_i and v_i are the position and velocity of the ith vehicle, respectively. The propelling force u_i represents the control input. Once u_i is appropriately chosen, the vehicular platoon is capable of achieving the desired spacing, maintaining an identical speed, and performing synchronous braking maneuvers. It is assumed that an inner-loop automatic controller exists in each vehicle for responding to the control input u_i.

2.3. Intervehicle Spacing Policy. The intervehicle spacing policy plays a vital role in the vehicular platoon control. In contrary, to track the speed of the leader vehicle and realize the predefined formation geometry, the objective of the vehicular platoon control is governed by the intervehicle policy:

$$\begin{cases} r_i(t) \longrightarrow r_j(t) + d_{ij}, \\ v_i(t) \longrightarrow v_0(t), \end{cases} \quad i \in \mathscr{V}, \tag{4}$$

where d_{ij} is the desired intervehicle spacing between the ith vehicle and the jth vehicle. It is assumed that $d_{ij} = -d_{ji}$. The formation geometry of the vehicular platoon is determined by d_{ij}. There are two main kinds of intervehicle spacing policies, *i.e.*, constant distance (CD) policy and constant time head headway (CTH) policy. For the CD policy, d_{ij} is set to be a constant number:

$$d_{ij} = (j - i)d_{i-1,i} = (j - i)d_0, \quad i \in \mathscr{V}, \tag{5}$$

where d_0 is the constant spacing between the ith vehicle and its preceding vehicle.

For the CTH policy, $d_{i-1,i}$ is dependent on the vehicle velocity v_i:

$$d_{i-1,i} = h \cdot v_i + d_0, \quad i \in \mathscr{V}, \tag{6}$$

where h is the constant time headway.

In accordance with some geometrical considerations, the spacing policy $d_{i-1,i}$ can be recast into the spacing with respect to the leader vehicle as $d_{ij} = d_{i0} - d_{j0}$. Thus, the objective of the platoon control in (4) can be rewritten as follows:

$$\begin{cases} r_i(t) \longrightarrow r_0(t) + d_{i0}, \\ v_i(t) \longrightarrow v_0(t), \end{cases} \quad i \in \mathscr{V}, \tag{7}$$

where d_{i0} is the desired distance from the leader to the ith vehicle.

2.4. Distributed Controller for the Vehicular Platoon with Time Delay. Nowadays, most literatures focus on designing the controller for the vehicular platoon without time delay [21, 22], and the distributed controller is designed as follows:

$$u_i(t) = -k_r \sum_{j=0}^{N} a_{ij}\left[r_i(t) - r_j(t) - d_{ij}\right] - k_v \sum_{j=0}^{N} a_{ij}\left[v_i(t) - v_j(t)\right], \tag{8}$$

where $k_r > 0$ and $k_v > 0$ are the control gains for the position and velocity, respectively.

However, due to the limited band width and congestion of the communication channels, the time delay inevitably appears in the vehicular platoon. Meanwhile, the time delay is the inherent phenomenon in the wireless communication networks, which is universally acknowledged as the main factor for the performance of the vehicular platoon, leading to the string instability. Therefore, by considering the time delay into the interconnected information flow, the distributed controller for the vehicular platoon with time delay can be designed as

$$u_i(t) = -k_r \sum_{j=0}^{N} a_{ij}\left[r_i(t-\tau) - r_j(t-\tau) - d_{ij}\right] - k_v \sum_{j=0}^{N} a_{ij}\left[v_i(t-\tau) - v_j(t-\tau)\right], \tag{9}$$

where τ represents the time delay. Generally, clock synchronization is guaranteed throughout the platoon via GPS [23], so the value of τ can be computed out according to the transmission time.

3. Time Delay Stability Margin for the Automated Vehicular Platoon

In this part, we aim to compute the time delay stability margin for the automated vehicular platoon under both undirected and directed topologies. To obtain the time delay stability margin, it is necessary to elaborately analyse the closed-loop system of the vehicular platoon. Besides, to compute the exact time delay stability margin, it is essential to obtain the necessary and sufficient condition. Furthermore, it is revealed that the exact time delay stability margin is determined by the largest eigenvalue, and a more rapid method for computing the exact time delay stability margin is proposed for the undirected topology.

3.1. Stability Analysis for the Automated Vehicular Platoon. To analyse the stability of system (3) with the distributed controller (9), the error states, which is determined with the comparison of the state information for the leader vehicle, is defined as follows:

$$\tilde{r} = \left[\tilde{r}_1, \tilde{r}_2, \ldots, \tilde{r}_N\right]^{\mathrm{T}}, \quad \tilde{v} = \left[\tilde{v}_1, \tilde{v}_2, \ldots, \tilde{v}_N\right]^{\mathrm{T}}, \tag{10}$$

where $\tilde{r}_i = r_i(t) - r_0(t) - d_{i0}$ is the spacing error state and $\tilde{v}_i = v_i(t) - v_0(t)$ is the velocity error state. $r_0(t)$ and $v_0(t)$ represent the position and velocity of the leader vehicle.

By substituting the error states into the distributed controller (9), it can be recast in terms of the error states as

$$u_i(t) = -k_r \sum_{j=0}^{N} a_{ij}\left[\tilde{r}_i(t-\tau) - \tilde{r}_j(t-\tau)\right] - k_v \sum_{j=0}^{N} a_{ij}\left[\tilde{v}_i(t-\tau) - \tilde{v}_j(t-\tau)\right]. \tag{11}$$

Therefore, by using the error dynamics (11), system (3) can be rewritten as follows:

$$\begin{cases} \dot{\tilde{r}}_i = \tilde{v}_i(t), \\ \dot{\tilde{v}}_i = -k_r \sum_{j=0}^{N} a_{ij}\left[\tilde{r}_i(t-\tau) - \tilde{r}_j(t-\tau)\right] \\ \quad -k_v \sum_{j=0}^{N} a_{ij}\left[\tilde{v}_i(t-\tau) - \tilde{v}_j(t-\tau)\right]. \end{cases} \tag{12}$$

For simplicity, we define the error state vector as $\tilde{x} = [\tilde{r}^{\mathrm{T}}, \tilde{v}^{\mathrm{T}}]^{\mathrm{T}}$. Then, the collective closed-loop dynamics of the vehicular platoon are rewritten into a compact form as follows:

$$\dot{\tilde{x}} = A\tilde{x} + B\tilde{x}(t-\tau), \tag{13}$$

with

$$A = \begin{bmatrix} 0_{N\times N} & I_{N\times N} \\ 0_{N\times N} & 0_{N\times N} \end{bmatrix}, \quad B = \begin{bmatrix} 0_{N\times N} & 0_{N\times N} \\ -k_r(\mathscr{L}+\mathscr{P}) & -k_v(\mathscr{L}+\mathscr{P}) \end{bmatrix}, \tag{14}$$

where $I_{N\times N}$ and $0_{N\times N}$ denote the N-dimensional identity matrix and zero matrix, respectively.

So far, the closed-loop dynamics of the vehicular platoon is build. In the following, the stability analysis will be implemented according to the augmented Laplacian matrix.

Therein, we define the eigenvalue of the augmented Laplacian matrix $\mathscr{L} + \mathscr{P}$ as $\lambda_i, i \in \mathscr{V}$, which mathematically reflects the important features of the augmented graph $\widetilde{\mathscr{G}}$. By utilizing the eigenvalue λ_i, it is convenient to analyse the stability of the closed-loop dynamics (13). Moreover, to facilitate the stability analysis of the closed-loop dynamics (13), we utilize the method in [24] to divide the entire vehicular platoon into some small synchronous subsystems.

Then, the characteristic equation of system (13) is given by

$$\det\left(sI - A - Be^{-\tau s}\right) = \prod_{i=1}^{N} f_i(s) = 0, \tag{15}$$

where

$$f_i(s) = s^2 + \left(k_v s + k_r\right)\lambda_i e^{-\tau s}. \tag{16}$$

Before analysing the stability of the closed-loop dynamics (13), some lemmas are provided as follows.

Lemma 1. *When the augmented graph $\widetilde{\mathscr{G}}$ contains a spanning tree, all the eigenvalues of $\mathscr{L} + \mathscr{P}$ are located in the open right half complex plane, i.e., $\lambda_i > 0, i \in \mathscr{V}$.*

Lemma 1 describes the distribution of the eigenvalues of $\mathscr{L}+\mathscr{P}$, and it is fundamental to indicate the stability and compute the exact time delay stability margin from the augmented graph $\widetilde{\mathscr{G}}$.

Lemma 2. *When the graph $\mathscr{G}$ is undirected, all the eigenvalues of $\mathscr{L}+\mathscr{P}$ are positive real numbers, i.e., $\lambda_i \in \mathbb{R}^+, i \in \mathscr{V}$.*

Lemma 2 describes the special character of undirected topologies. When the interconnected information flow among the follower vehicles is undirected, it is useful to simplify the theoretical deduction of verifying the stability. The proof of Lemma 1 and 2 can be found in [21].

Lemma 3. *The closed-loop dynamics (13) are asymptotically stable if and only if every equation (16) is Hurwitz stable, i.e., the roots of the closed-loop system's characteristic equation are all located in the open left half complex plane.*

Based on the abovementioned three lemmas, we obtain the first stability result for the closed-loop dynamics (13).

Theorem 1. *If the closed-loop dynamics (13) is asymptotically stable, the following inequality holds:*

$$\frac{k_v^2}{k_r} > \max_{i\in\mathscr{V}} \frac{\mathrm{Im}^2(\lambda_i)}{\mathrm{Re}(\lambda_i)|\lambda_i|^2}, \tag{17}$$

where $|\lambda_i|$ is the module of λ_i. $Re(\lambda_i)$ and $Im(\lambda_i)$ are the real part and imaginary part of λ_i, respectively.

Proof. The closed-loop dynamics (13) should be primarily stable for the delay-free case [25]. When $\tau = 0$, there exists

$$f_i(s) = s^2 + (k_v s + k_r)\lambda_i = 0. \tag{18}$$

As $\lambda_i = \mathrm{Re}(\lambda_i) + \iota \cdot \mathrm{Im}(\lambda_i), \iota^2 = -1$ is probably a complex number, (18) is transformed into a fourth-order equation as

$$s^4 + 2k_v\mathrm{Re}(\lambda_i)s^3 + \left[k_v^2|\lambda_i|^2 + 2k_r\mathrm{Re}(\lambda_i)\right]s^2 + 2k_rk_v|\lambda_i|^2 s + k_r^2|\lambda_i|^2 = 0. \tag{19}$$

Then, the stability of (19) is examined based on the Routh–Hurwitz stability criterion:

$$\begin{bmatrix} s^4 & 1 & k_v^2|\lambda_i|^2 + 2k_r\mathrm{Re}(\lambda_i) & k_r^2|\lambda_i|^2 \\ s^3 & 2k_v\mathrm{Re}(\lambda_i) & 2k_rk_v|\lambda_i|^2 & \\ s^2 & \dfrac{k_v^2\mathrm{Re}(\lambda_i)|\lambda_i|^2 + k_r\mathrm{Re}^2(\lambda_i) - k_r\mathrm{Im}^2(\lambda_i)}{\mathrm{Re}(\lambda_i)} & k_r^2|\lambda_i|^2 & \\ s^1 & \dfrac{2k_rk_v|\lambda_i|^2\left[k_v^2\mathrm{Re}(\lambda_i)|\lambda_i|^2 - k_r\mathrm{Im}^2(\lambda_i)\right]}{k_v^2\mathrm{Re}(\lambda_i)|\lambda_i|^2 + k_r\mathrm{Re}^2(\lambda_i) - k_r\mathrm{Im}^2(\lambda_i)} & & \\ s^0 & k_r^2|\lambda_i|^2 & & \end{bmatrix}. \tag{20}$$

The Routh table is listed out in equation (20). Considering the definition that $k_r > 0, k_v > 0$ in (9) and the fact that $\mathrm{Re}(\lambda_i) > 0$ from Lemma 1, it is concluded that (18) is asymptotically stable if and only if

$$\frac{k_v^2}{k_r} > \frac{\mathrm{Im}^2(\lambda_i)}{\mathrm{Re}(\lambda_i)|\lambda_i|^2}. \tag{21}$$

Taking all λ_i into consideration, if the closed-loop dynamics (13) are asymptotically stable, inequality (17) holds. □

Remark 1. The stability condition (17) of Theorem 1 is a necessary and sufficient condition of the closed-loop dynamics (13) for the delay-free case, but it is just a necessary condition for the delay case. For $\tau > 0$, the stability of the closed-loop dynamics (13) is not only correlated with the control gains and structure of the interconnected information flow but also dependent on the time delay.

Corollary 1. *For $\tau = 0$, when the graph $\mathscr{G}$ is undirected, the closed-loop dynamics (13) are asymptotically stable, for any $k_r > 0, k_v > 0$.*

When the graph $\mathscr{G}$ is undirected, there exists $\mathrm{Im}(\lambda_i) = 0$ according to Lemma 2. Hence, inequality (17) holds for any $k_r > 0, k_v > 0$.

3.2. Computation of the Exact Time Delay Stability Margin for the Automated Vehicular Platoon. For the delay case $\tau > 0$, we review the characteristic equation (16) as

$$f_i(s) = s^2 + (k_v s + k_r)\lambda_i e^{-\tau s}. \tag{22}$$

It is obvious that $f_i(s), i \in \mathscr{V}$ is a quasi-polynomial and its characteristic equation $f_i(s) = 0$ is a transcendental equation. Hence, it is complicated to analyse the roots of the characteristic equation. Despite of this, we are still devoted to checking the property of the roots to find the exact time delay stability margin.

Theorem 2. *For the closed-loop dynamics (13) satisfying condition (17), let $\omega_i > 0$ be the root of the following equation:*

$$\omega_i^4 - k_v^2|\lambda_i|^2\omega_i^2 - k_r^2|\lambda_i|^2 = 0, \tag{23}$$

with $\omega_i = \sqrt{(k_v^2|\lambda_i|^2 + \sqrt{k_v^4|\lambda_i|^4 + 4k_r^2|\lambda_i|^2})}$. *Take*

$$\tau_i = \frac{\arctan\xi_i + k\pi}{\omega_i}, \quad k \in \{0, 1\}, \tag{24}$$

where $\xi_i = -(\delta_i/\theta_i)$ *with* $\delta_i = k_v\omega_i Re(\lambda_i) + k_r Im(\lambda_i)$ *and* $\theta_i = k_v\omega_i Im(\lambda_i) - k_r Re(\lambda_i)$. *Let* $\tau_{min} = \min_{i\in\mathscr{V}}\tau_i$. *Then, system (13) is asymptotically stable if and only if* $\tau \in [0, \tau_{min})$.

Proof. According to Corollary 2.4 in [26], it is known that for a quasi-polynomial $g(s, e^{-\tau s}) = g_0(s) + g_1(s)e^{-\tau s}$, if $g(s, e^{-\tau s})$ is Hurwitz stable for $\tau = 0$ and unstable for $\tau > \tau_{\min}$, there must exist a root on the imaginary axis for $g(s, e^{-\tau_{\min} s})$. In our work, if the stability condition (17) in Theorem 1 is satisfied, $f_i(s)$ in (22) is Hurwitz stable for $\tau = 0$. Thus, it is available to utilize Corollary 2.4 in [26] to find the exact time delay stability margin $\tau_{\min}$. Afterwards, we aim to find the root $\iota \cdot \omega_i$ on the imaginary axis for τ_i.

With respect to the imaginary root $\iota \cdot \omega_i$, there exists $f_i(\iota \cdot w_i) = 0$, which implies that both the real and imaginary parts of $f_i(\iota \cdot w_i)$ are zero, shown as

$$\begin{cases} -\omega_i^2 + \delta_i \sin(\tau_i\omega_i) - \theta_i \cos(\tau_i\omega_i) = 0, \\ \theta_i \sin(\tau_i\omega_i) + \delta_i \cos(\tau_i\omega_i) = 0. \end{cases} \tag{25}$$

By rearranging (25), two following trigonometric functions are obtained:

$$\begin{cases} \sin(\tau_i\omega_i) = \dfrac{\theta_i\omega_i^2}{\delta_i^2 + \theta_i^2}, \\ \cos(\tau_i\omega_i) = -\dfrac{\delta_i\omega_i^2}{\delta_i^2 + \theta_i^2}, \end{cases} \tag{26}$$

where $\delta_i^2 + \theta_i^2 = (k_v^2\omega_i^2 + k_r^2)|\lambda_i|^2$. According to the well-known trigonometric property $\sin^2(\tau_i\omega_i) + \cos^2(\tau_i\omega_i) = 1$, it is concluded that

$$\omega_i^4 - k_v^2|\lambda_i|^2\omega_i^2 - k_r^2|\lambda_i|^2 = 0. \tag{27}$$

Then, two real-valued roots about ω_i, which are positive and negative, respectively, can be solved out. Meanwhile, it is obtained that $\xi_i = \tan(\tau_i\omega_i) = (\sin(\tau_i\omega_i)/\cos(\tau_i\omega_i)) = (-(\theta_i/\delta_i))$ based on (26). The delay for $i \in \mathscr{V}$ is also deduced as $\tau_i = (\arctan\xi_i + k\pi)/\omega_i, k \in \{0, 1\}$, where the integer k should be chosen as the minimum value satisfying $\tau_i > 0$.

Next, we aim to demonstrate that only the situation $\omega_i > 0$ needs to be considered. Two cases for the graph $\mathscr{G}$, *i.e.*, undirected and directed topologies, are taken into account as follows:

(i) The undirected graph $\mathscr{G}$: in this case, $\mathrm{Im}(\lambda_i) = 0$. We assume that the two real-valued roots of (27) are ω_{i1}, ω_{i2}, and $\omega_{i1} > 0, \omega_{i2} < 0$. It is obvious that $\omega_{i2} = -\omega_{i1}$. Based on this, one can find that $\delta_{i2} = -\delta_{i1}, \theta_{i2} = \theta_{i1}$, and $\xi_{i2} = -\xi_{i1}$. There must exist $\arctan\xi_{i2}/\omega_{i2} = \arctan\xi_{i1}/\omega_{i1}$ such that we can simply take $\tau_{i2} = \tau_{i1}$. In a word, considering only the positive root $\omega_i > 0$ suffices to obtain τ_i, because the imaginary roots for $f_i(s)$ form complex conjugate pairs.

(ii) The directed graph $\mathscr{G}$: in this case, $\mathrm{Im}(\lambda_i) \neq 0$. There must also exist a conjugate eigenvalue of λ_i for the directed graph $\mathscr{G}$, where the conjugate eigenvalue is also a root of (27). We define the conjugate eigenvalue as $\lambda_l = \mathrm{Re}(\lambda_i) - \iota \cdot \mathrm{Im}(\lambda_i), l \in \mathscr{V}$. Let $\omega_{i1} > 0, \omega_{i2} < 0, \omega_{l1} > 0$, and $\omega_{l2} < 0$. According to (27), it is easy to see that $\omega_{l1} = \omega_{i1}$ and $\omega_{l2} = \omega_{i2}$. Then, one can find that $\delta_{l2} = -\delta_{i1}, \theta_{l2} = \theta_{i1}$, and $\xi_{l2} = -\xi_{i1}$. There must exist $\arctan\xi_{l2}/\omega_{l2} = \arctan\xi_{i1}/\omega_{i1}$ such that we can simply take $\tau_{l2} = \tau_{i1}$. Therefore, for the directed graph $\mathscr{G}$, considering only the positive root $\omega_i > 0$ still suffices to obtain τ_i.

Then, by synthesizing the above two cases with the fact that $\omega_i > 0$, the positive root of (27) is solved out as follows:

$$\omega_i = \sqrt{\left(k_v^2|\lambda_i|^2 + \sqrt{k_v^4|\lambda_i|^4 + 4k_r^2|\lambda_i|^2}\right)}. \tag{28}$$

At last, we scan all the eigenvalue $\lambda_i, i \in \mathscr{V}$ to compute all τ_i and find the exact time margin $\tau_{\min} = \min_{i\in\mathscr{V}}\tau_i$. □

Remark 2. Theorem 2 provides a method for finding the exact time delay stability margin $\tau_{\min}$ of the closed-loop dynamics (13). Theorem 2 is a necessary and sufficient condition for the stability for the delay case.

3.3. A Rapid Method for Computing the Exact Time Delay Stability Margin under the Undirected Topology. A large-scale vehicular platoon generally generates plenty of eigenvalues of the graph $\mathscr{G}$. It is time consuming to scan all the eigenvalue $\lambda_i, i \in \mathscr{V}$ to compute all τ_i. However, it is common knowledge that the most critical eigenvalue directly determines the exact time delay stability margin. If the most critical eigenvalue is found, there is no need to scan all the other eigenvalues. Moreover, because it is very fussy to analyse the most critical eigenvalue for the directed graph, we only consider the undirected topology. Therefore, we focus on look for the most critical eigenvalue under the undirected topology, aiming to reduce the computational burden and quickly compute the exact time delay stability margin.

Theorem 3. *For the closed-loop dynamics (13), under the undirected graph $\mathscr{G}$, let $\lambda_{\max} = \max_{i\in\mathscr{V}}\lambda_i$. Then, $\lambda_{\max}$ is the most critical eigenvalue, which determines the exact time delay stability margin τ_{min}.*

Proof. Although it is difficult to directly confirm whether the monotonicity of τ_i depends on the monotonicity of λ_i, we plan to reveal their monotonous relationship through two steps. By treating ω_i as an immediate variable, the first step is to verify that the monotonicity of ω_i depends on the

monotonicity of λ_i, and the second step is to verify that the monotonicity of τ_i depends on the monotonicity of ω_i.

In the first step, we only consider the case $\omega_i > 0$ in accordance with Theorem 2. When the graph $\mathcal{G}$ is undirected, (28) turns into the following form as follows:

$$\omega_i = \sqrt{\frac{1}{2}\left(k_v^2\lambda_i^2 + \sqrt{k_v^4\lambda_i^4 + 4k_r^2\lambda_i^2}\right)}. \tag{29}$$

According to Lemma 2, λ_i is a positive real number for the undirected topology, so it can be seen that ω_i gets larger with the increase of λ_i. Then, it is demonstrated that the monotonicity of the immediate variable ω_i depends on the monotonicity of λ_i.

In the second step, we aim to verify that the monotonicity of τ_i depends on the monotonicity of ω_i. with respect to (24), there exists $\tau_i = \omega_i^{-1}\arctan\xi_i = \omega_i^{-1}\arctan(k_v\omega_i/k_r)$ with $\omega_i > 0$. We intend to apply the partial derivative property to conform the monotonicity. The partial derivative $(\partial\tau_i/\partial\omega_i)$ is calculated as follows:

$$\begin{aligned}\frac{\partial\tau_i}{\partial\omega_i} &= -\frac{1}{\omega_i^2}\arctan\frac{k_v\omega_i}{k_r} + \frac{1}{\omega_i}\cdot\frac{k_rk_v}{k_r^2 + k_v^2\omega_i^2} \\ &= \frac{1}{\omega_i^2}\left[-\arctan\frac{k_v\omega_i}{k_r} + \omega_i\cdot\frac{k_rk_v}{k_r^2 + k_v^2\omega_i^2}\right],\end{aligned} \tag{30}$$

with $(\partial\arctan(k_v\omega_i/k_r)/\partial\omega_i) = (k_rk_v/k_r^2 + k_v^2\omega_i^2)$.

In (30), the term $\arctan(k_v\omega_i/k_r)$ still exists. Therefore, it is uneasy to identify whether (30) is positive or negative. To solve this problem, we deduce the partial derivative once again, and an auxiliary function is given by

$$\mathrm{d}(\omega_i) = -\arctan\frac{k_v\omega_i}{k_r} + \omega_i\cdot\frac{k_rk_v}{k_r^2 + k_v^2\omega_i^2}. \tag{31}$$

Comparing with (31), (30) can be rewritten as

$$\frac{\partial\tau_i}{\partial\omega_i} = \frac{1}{\omega_i^2}\mathrm{d}(\omega_i). \tag{32}$$

Then, the partial derivative $(\partial\mathrm{d}(\omega_i)/\partial\omega_i)$ is calculated as

$$\begin{aligned}\frac{\partial\mathrm{d}(\omega_i)}{\partial\omega_i} &= -\frac{k_rk_v}{k_r^2 + k_v^2\omega_i^2} + \frac{k_r^3k_v - k_rk_v^3\omega_i^2}{\left(k_r^2 + k_v^2\omega_i^2\right)^2} \\ &= \frac{-2k_rk_v^3\omega_i^2}{\left(k_r^2 + k_v^2\omega_i^2\right)^2}.\end{aligned} \tag{33}$$

With the definition that $k_r > 0, k_v > 0$ in (9), it is noted that $(\partial\mathrm{d}(\omega_i)/\partial\omega_i) = 0$ when $\omega_i = 0$, and $(\partial\mathrm{d}(\omega_i)/\partial\omega_i) < 0$ when $\omega_i > 0$. Then, it is concluded that $(\partial\tau_i/\partial\omega_i) < 0$ in (32) when $\omega_i > 0$, which means that τ_i gets smaller with the increase of ω_i. Until now, we verify that the monotonicity of τ_i depends on that of ω_i by using the partial derivative property.

By taking the abovementioned two steps into account, it is confirmed that τ_i gets smaller with the increase of λ_i. Hence, the largest eigenvalue $\lambda_{\max}$ is most critical and determines the exact time delay stability margin $\tau_{\min}$. □

Remark 3. Theorem 3 reveals the inherent relationship between the exact time delay stability margin and the eigenvalues of the augmented Laplacian matrix for the undirected graph $\mathcal{G}$. According to Theorem 3, just computing one delay corresponding to the largest eigenvalue $\lambda_{\max}$ suffices to obtain the exact time delay stability margin, and it is no longer necessary to scan the other eigenvalues. For the large-scale vehicular platoon, utilizing Theorem 3 can dramatically reduce the computational burden.

4. Numerical Simulations

In this section, numerical simulations are conducted to verify the effectiveness of the main results. Therein, an automated vehicular platoon with five identical vehicles (one leader and four followers) is considered. Simulations are performed for a single-lane road. As the intelligent transportation system scenario described in [27], we take the structure of the interconnected information flow that the leader vehicle transmits to the follower vehicles. The pinning matrix is set as $\mathcal{P} = \mathrm{diag}\{1, 0, 1, 0\}$. Meanwhile, the follower vehicles share the state information with their neighbouring vehicles and form undirected topology or directed topology (as depicted in Figure 1). It is noted that the configuration of the interconnected information flow contains a spanning tree and satisfies Lemma 1. The leader vehicle maneuvers at a constant velocity of 20 m/s (*i.e.*, 72 km/h). The CD policy is chosen as the intervehicle spacing policy, and the desired spacing is set as $d_{ij} = 15$ m. The initial error states are defined as $\tilde{r}(0) = [5, -5, 10, -10]^{\mathrm{T}}$ m and $\tilde{v}(0) = [-2, 2, -4, 4]^{\mathrm{T}}$ m/s. In the following, two scenarios, undirected and directed topologies, are simulated for investigating the stability and the exact time delay stability margin.

4.1. Undirected Topology. For an undirected topology, the numerical simulations are conducted to verify the effectiveness of Theorem 2 and Theorem 3. The adjacency matrix $\mathcal{A}$ and the Laplacian matrix $\mathcal{L}$ are given by

$$\begin{aligned}\mathcal{A} &= \begin{bmatrix}0 & 1 & 0 & 0\\ 1 & 0 & 1 & 0\\ 0 & 1 & 0 & 1\\ 0 & 0 & 1 & 0\end{bmatrix}, \\ \mathcal{L} &= \begin{bmatrix}1 & -1 & 0 & 0\\ -1 & 2 & -1 & 0\\ 0 & -1 & 2 & -1\\ 0 & 0 & -1 & 1\end{bmatrix}.\end{aligned} \tag{34}$$

The eigenvalues of the augmented Laplacian matrix $\mathcal{P} + \mathcal{L}$ for the undirected topology are $\lambda_1 = 0.382$, $\lambda_2 = 1.000$, $\lambda_3 = 2.618$, and $\lambda_4 = 4.000$. It is seen that all the eigenvalues are positive real numbers such that their distribution coincides with Lemma 2. The control gains are tuned as $k_r = 1$ and $k_v = 1$ satisfying Theorem 1. We scan every eigenvalue to get that $\tau_1 = 0.88$ s, $\tau_2 = 0.71$ s, $\tau_3 = 0.44$ s, and $\tau_4 = 0.32$ s. Then, the exact time delay stability margin

$\tau_{\min} = 0.32$ s is obtained. One can find that the exact time delay stability margin is determined by the largest eigenvalue $\lambda_4 = 4.000$, which confirms to the conclusion of Theorem 3. Two extreme cases are verified with the time delays $\tau = 0.31$ s and $\tau = 0.33$ s, which are depicted in Figures 2 and 3, respectively. It is seen that the stability is guaranteed in Figure 2 and instability occur in Figure 3. Thus, the simulation results under undirected topology support the main results of Theorems 2 and 3.

4.2. Directed Topology. For a directed topology, the numerical simulations are conducted to verify the effectiveness of Theorem 2. The adjacency matrix $\mathscr{A}$ and the Laplacian matrix $\mathscr{L}$ are given by

$$\mathscr{A} = \begin{bmatrix} 0 & 0 & 0 & 1 \\ 1 & 0 & 0 & 0 \\ 1 & 0 & 0 & 0 \\ 0 & 0 & 1 & 0 \end{bmatrix}, \quad \mathscr{L} = \begin{bmatrix} 1 & 0 & 0 & -1 \\ -1 & 1 & 0 & 0 \\ -1 & 0 & 1 & 0 \\ 0 & 0 & -1 & 1 \end{bmatrix}. \tag{35}$$

The eigenvalues of the augmented Laplacian matrix $\mathscr{P} + \mathscr{L}$ for directed topology are $\lambda_1 = 1.000$, $\lambda_2 = 2.233 + 0.793\iota$, $\lambda_3 = 2.233 - 0.793\iota$, and $\lambda_4 = 0.534$. It is seen that all the eigenvalues have positive real parts such that their distribution coincides with Lemma 1. The control gains are tuned as $k_r = 1$ and $k_v = 1$ satisfying Theorem 1. We scan every eigenvalue to get that $\tau_1 = 0.71$ s, $\tau_2 = 0.60$ s, $\tau_3 = 0.34$ s, and $\tau_4 = 0.83$ s. Then, the exact time delay stability margin $\tau_{\min} = 0.34$ s is obtained. Two extreme cases are verified with the time delays $\tau = 0.33$ s and $\tau = 0.35$ s, which are depicted in Figures 4 and 5, respectively. It is seen that the stability is guaranteed in Figure 4 and instability occurs in Figure 5. Thus, the simulation results under directed topology support the main results of Theorem 2.

Furthermore, it is noted that the exact time delay stability margin for directed topology in this example is associated with one of the eigenvalues with the largest module. This is an interesting phenomenon. Therefore, our further research topic is to figure out whether this phenomenon is general for directed topologies. Meanwhile, this paper focuses on computing the exact time delay stability margin for linear dynamical systems. The proposed method is only suitable for linear dynamical systems because we obtain the exact time delay stability margin according to the characteristic equation of the closed-loop system. The method cannot be directly applied to nonlinear dynamical systems. However, it can be extended to the nonlinear dynamical systems which can be converted into controllable linear systems via dynamic feedback linearisation. Therefore, finding exact time delay stability margin for nonlinear dynamical systems is our another work in the future.

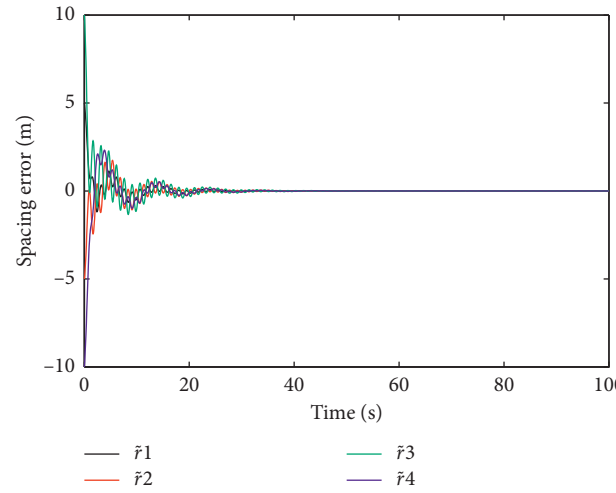

Figure 2: Spacing errors for an automated vehicular platoon under undirected topology with $\tau = 0.31$ s.

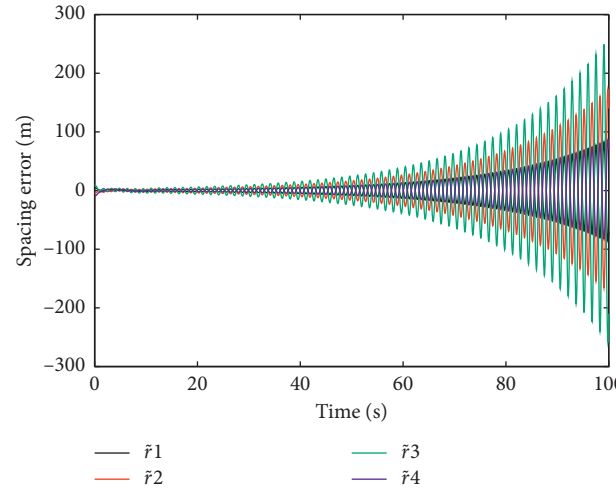

Figure 3: Spacing errors for an automated vehicular platoon under undirected topology with $\tau = 0.33$ s.

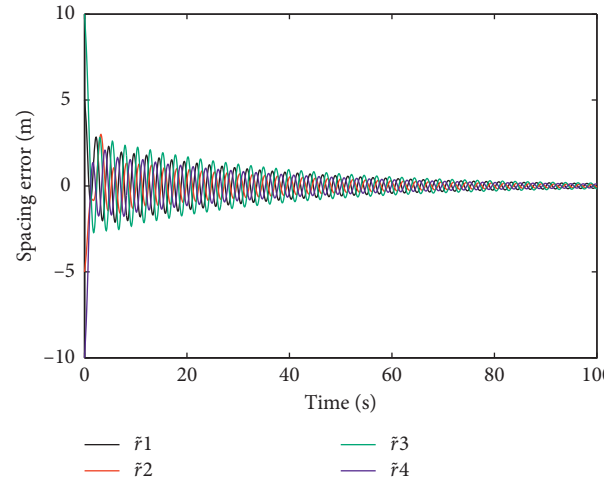

Figure 4: Spacing errors for an automated vehicular platoon under directed topology with $\tau = 0.33$ s.

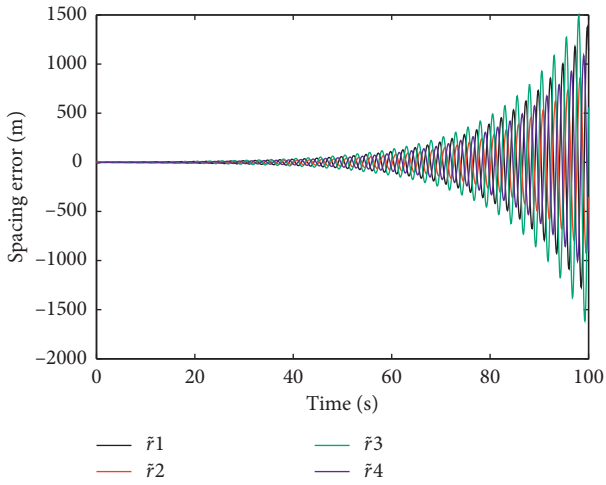

Figure 5: Spacing errors for an automated vehicular platoon under directed topology with $\tau = 0.35$ s.

5. Conclusions

This paper investigates the problem of finding the exact time delay margin for the automated vehicular platoon. After designing a distributed controller, we focus on analysing the stability of the entire platoon. By investigating the roots' distribution of the closed-loop system's characteristic equation, the exact time delay stability margin is acquired. It is a necessary and sufficient condition, which implies that our result outperforms most existing methods at overcoming conservatism. Furthermore, a rapid method for finding the exact time delay stability margin for undirected topologies is proposed by exploring the monotonicity relationship between each eigenvalue of the augmented Laplacian matrix and its corresponding delay. We analytically demonstrate that the largest eigenvalue determines the exact time delay stability margin. Therefore, it is no longer necessary to compute the delays corresponding to the other eigenvalues. For the large-scale vehicular platoon, utilizing our proposed theorem can dramatically reduce the computational burden. Numerical simulations for undirected and directed topologies are both conducted to verify the effectiveness of the theoretical derivation. Simulation results additionally show that the exact time delay stability margin for directed topologies is associated with one of the eigenvalues with the largest module. Figuring out, whether this interesting phenomenon is general, is the subject of our ongoing work.

Data Availability

The data used to support the findings of this study are available from the corresponding author upon request.

Conflicts of Interest

Xunxun Zhang received the M.S. degree in control theory and control engineering from Northwestern Polytechnical University, China, in 2012. She received the Ph.D. degree in transportation information engineering and control from Chang'an University, China, in 2018. She is now working in the School of Civil Engineering, Xi'an University of Architecture & Technology, China. Her research interest covers modeling, analysis and control of flocking system, multi-robot formation control, and automated vehicular platoon control. Li Li received the M.S. degree in control theory and control engineering from Northwestern Polytechnical University, China, in 2003. She received the Ph.D. degree in Computer Science and Technology, Tsinghua University, China, in 2008. She is currently working in the College of Computer and Information Engineering, Tianjin Normal University, China. Her research interest includes intelligent control, fuzzy systems, and adaptive control. Xu Zhu received the M.S. and Ph.D. degrees in control theory and control engineering from Northwestern Polytechnical University, China, 2014, respectively. He is currently an Associate Professor with the School of Electronic and Control Engineering, Chang'an University. His research interest includes multi-UAV cooperative control, automated vehicular platoon control, and fight control.

Acknowledgments

This work was supported in part by the China Postdoctoral Science Foundation under Grant 2017M613030.

References

[1] D. Jia, K. Lu, J. Wang, X. Zhang, and X. Shen, "A survey on platoon-based vehicular cyber-physical systems," *IEEE Communications Surveys & Tutorials*, vol. 18, no. 1, pp. 263–284, 2016.

[2] K. C. Dey, L. Yan, X. Wang et al., "A review of communication, driver characteristics, and controls aspects of cooperative adaptive cruise control (cacc)," *IEEE Transactions on Intelligent Transportation Systems*, vol. 17, no. 2, pp. 491–509, 2016.

[3] S. E. Li, Y. Zheng, K. Li, L. Y. Wang, and H. Zhang, "Platoon control of connected vehicles from a networked control perspective: literature review, component modeling, and controller synthesis," *IEEE Transactions on Vehicular Technology*, p. 1, 2018.

[4] S. E. Shladover, C. A. Desoer, J. K. Hedrick et al., "Automated vehicle control developments in the path program," *IEEE Transactions on Vehicular Technology*, vol. 40, no. 1, pp. 114–130, 1991.

[5] J. Zhang, F.-Y. Wang, K. Wang, W.-H. Lin, X. Xu, and C. Chen, "Data-driven intelligent transportation systems: a survey," *IEEE Transactions on Intelligent Transportation Systems*, vol. 12, no. 4, pp. 1624–1639, 2011.

[6] S. Santini, A. Salvi, A. S. Valente, A. Pescapè, M. Segata, and R. L. Cigno, "A consensus-based approach for platooning with inter-vehicular communications," in *Proceedings of the IEEE Conference on Computer Communications*, pp. 1158–1166, IEEE, Kowloon, Hong Kong, April 2015.

[7] S. S. Stankovic, M. J. Stanojevic, and D. D. Siljak, "Decentralized overlapping control of a platoon of vehicles," *IEEE Transactions on Control Systems Technology*, vol. 8, no. 5, pp. 816–832, 2000.

[8] P. Seiler, A. Pant, and K. Hedrick, "Disturbance propagation in vehicle strings," *IEEE Transactions on Automatic Control*, vol. 49, no. 10, pp. 1835–1841, 2004.

[9] L. Xu, L. Y. Wang, G. Yin, and H. Zhang, "Communication information structures and contents for enhanced safety of highway vehicle platoons," *IEEE Transactions on Vehicular Technology*, vol. 63, no. 9, pp. 4206–4220, 2014.

[10] G. J. L. Naus, R. P. A. Vugts, J. Ploeg, M. J. G. van de Molengraft, and M. Steinbuch, "String-stable cacc design and experimental validation: a frequency-domain approach," *IEEE Transactions on Vehicular Technology*, vol. 59, no. 9, pp. 4268–4279, 2010.

[11] L. Li, D. Wen, and D. Yao, "A survey of traffic control with vehicular communications," *IEEE Transactions on Intelligent Transportation Systems*, vol. 15, no. 1, pp. 425–432, 2014.

[12] D. Jia and D. Ngoduy, "Platoon based cooperative driving model with consideration of realistic inter-vehicle communication," *Transportation Research Part C: Emerging Technologies*, vol. 68, pp. 245–264, 2016.

[13] A. Ghasemi, R. Kazemi, and S. Azadi, "Exact stability of a platoon of vehicles by considering time delay and lag," *Journal of Mechanical Science and Technology*, vol. 29, no. 2, pp. 799–805, 2015.

[14] M. Saeednia and M. Menendez, "A consensus-based algorithm for truck platooning," *IEEE Transactions on Intelligent Transportation Systems*, vol. 18, no. 2, pp. 404–415, 2017.

[15] A. Shariati and M. Tavakoli, "A descriptor approach to robust leader-following output consensus of uncertain multi-agent systems with delay," *IEEE Transactions on Automatic Control*, vol. 62, no. 10, pp. 5310–5317, 2017.

[16] A. Salvi, S. Santini, and A. S. Valente, "Design, analysis and performance evaluation of a third order distributed protocol for platooning in the presence of time-varying delays and switching topologies," *Transportation Research Part C: Emerging Technologies*, vol. 80, pp. 360–383, 2017.

[17] M. di Bernardo, A. Salvi, and S. Santini, "Distributed consensus strategy for platooning of vehicles in the presence of time-varying heterogeneous communication delays," *IEEE Transactions on Intelligent Transportation Systems*, vol. 16, no. 1, pp. 102–112, 2015.

[18] C.-L. Liu and Y.-P. Tian, "Formation control of multi-agent systems with heterogeneous communication delays," *International Journal of Systems Science*, vol. 40, no. 6, pp. 627–636, 2009.

[19] U. Münz, A. Papachristodoulou, and F. Allgöwer, "Delay robustness in consensus problems," *Automatica*, vol. 46, no. 8, pp. 1252–1265, 2010.

[20] X. F. Wang and G. Chen, "Pinning control of scale-free dynamical networks," *Physica A: Statistical Mechanics and Its Applications*, vol. 310, no. 3-4, pp. 521–531, 2002.

[21] Y. Zheng, S. E. Li, K. Li, and L.-Y. Wang, "Stability margin improvement of vehicular platoon considering undirected topology and asymmetric control," *IEEE Transactions on Control Systems Technology*, vol. 24, no. 4, pp. 1253–1265, 2016.

[22] P. Barooah and J. P. Hespanha, "Error amplification and disturbance propagation in vehicle strings with decentralized linear control," in *Proceedings of the European Control Conference, 44th IEEE Conference on Decision and Control*, pp. 4964–4969, IEEE, Seville, Spain, December 2005.

[23] J. Elson and K. Römer, "Wireless sensor networks," *ACM SIGCOMM Computer Communication Review*, vol. 33, no. 1, pp. 149–154, 2003.

[24] W. Hou, M. Fu, H. Zhang, and Z. Wu, "Consensus conditions for general second-order multi-agent systems with communication delay," *Automatica*, vol. 75, pp. 293–298, 2017.

[25] R. Cepeda-Gomez and N. Olgac, "Consensus analysis with large and multiple communication delays using spectral delay space concept," *International Journal of Control*, vol. 84, no. 12, pp. 1996–2007, 2011.

[26] S. Ruan and J. Wei, "On the zeros of transcendental functions with applications to stability of delay differential equations with two delays," *Dynamics of Continuous Discrete and Impulsive Systems Series A*, vol. 10, no. 6, pp. 863–874, 2003.

[27] E. Coelingh and S. Solyom, "All aboard the robotic road train," *IEEE Spectrum*, vol. 49, no. 11, pp. 34–39, 2012.